

PAPER • OPEN ACCESS

Behavior of Swelling Soil Treated by Grid Geocell Columns under a Tank Footing

To cite this article: Raid R. Al-Omari *et al* 2019 *IOP Conf. Ser.: Mater. Sci. Eng.* **579** 012041

View the [article online](#) for updates and enhancements.



IOP | ebooks™

Bringing you innovative digital publishing with leading voices to create your essential collection of books in STEM research.

Start exploring the collection - download the first chapter of every title for free.

Behavior of Swelling Soil Treated by Grid Geocell Columns under a Tank Footing

Raid R. Al-Omari¹, Mohammed Y. Fattah^{2#}, Haifaa A. Ali³

¹Professor, Civil Engineering Department, College of Engineering, Al-Nahrain University, Baghdad, Iraq.

²Professor, Building and Construction Engineering Department, University of Technology, Baghdad, Iraq.

³Lecturer, Civil Engineering Department, College of Engineering, University of Baghdad, Baghdad, Iraq.

#Corresponding author's e-mail address: myf_1968@yahoo.com.

Abstract. Fuel tanks usually induce large settlements due to heavy loading which requires treatment for the underlying soils. In this paper, a method of treating the swelling of expansive soil is presented. The method is simply based on the embedment of a geogrid (or a geomesh) in the soil. The geogrid is extended continuously inside the volume of soil where the swell is required to be controlled and orientated in the direction of swell. Soils with different swelling potentials were employed; bentonite-based Na and kaolinite mixed with bentonite. To investigate the swell, swell- partial shrinkage and other phenomena for untreated soils in comparison with their counterparts of treated soils, laboratory model tests were carried out in 800 × 200 mm box container and 600 mm in height. Swelling and cyclic wetting along with drying tests were carried out on each sample with pore water pressure measurement. Swelling test in the model reveals promising results of the proposed treatment technique. The improvement factors, range between 30% to 60 % depending on the geogrid stiffness, soil plasticity, fill material (sand or clay) and dry density of sand fill. The geocell has a significant effect on the experimental results. The reduction in swell increases with increasing the geogrid stiffness and when using sand as a fill material, the reduction is apparently due to a strong interference bond which restricts the relative movement between the clay and the grid. The use of geocell filled with the same expansive soil causes a decrease by about 19% and 42 % in the final swelling of soils, whereas filling the cell with sand causes about 35 % and 64 % reduction for the soils, respectively. The treatment method shows the activity of geocell fill material in reducing the matric suction (pore water pressure). When sand is used, a new channel is created for the dissipation of pore water pressure.

1. Introduction

Expansive soils are characterized as problematic as they exhibit swelling with absorption of water and shrinking with adsorption. Such volume changes caused by swelling and shrinkage movements often distress the infrastructure that is not designed to withstand these movements. In addition to swelling, shrinkage-related volume change is critical in influencing the overall volume



change properties of the soil. Field conditions that promote shrinkage or shrinkage-induced crack formation include environmental changes, construction process, and surcharge loading. Environmental changes include freezing (the growth of ice lenses), differential swelling (coupled with the weakening of interparticle forces during rapid wetting), and drying (shrinkage of clay mass) [1].

Many factors govern the expansion behavior of soil. The primary factors are the availability of moisture and the amount and type of the clay size particles in the soil. Factors affecting the expansion behavior include the type of soil (natural or fill), the condition of the soil in terms of dry density and moisture content, the magnitude of the surcharge pressure, the amount of non-expansive material (gravel-or cobble-size particles), and the amount of aging [2] [3]. In general, expansive potential increases as the dry density increases and the moisture content decreases. In addition, the expansion increases as the surcharge pressure decreases.

Using the enlarged oedometer, the improvement factor, IF, is defined as the difference between the final swell of unreinforced sample, W_u , and the final swell of the corresponding reinforced sample, W_r , divided by the final unreinforced swell, thus [4]:

$$IF = \frac{W_u - W_r}{W_u} \quad (1)$$

The value of W_r is corrected for the unreinforced length as the soil sample height is slightly larger than the geocell height.

The swell potential and swell pressure are dependent on several factors namely the type and amount of clay minerals present, the initial dry density (void ratio) and water content of the soil specimen, the nature of pore fluid, the type of exchangeable cations, the overburden pressure, and the wetting and drying effects [2] [3] [5]. The swell potential and swell pressure are known to increase with increasing of clay content and dry density and decrease with increasing of initial water content, overburden pressure, pore salt concentration, and exchangeable cation valence [2] [6]. However, clay soils in arid and semi-arid regions are subjected to cycles of wetting and drying in the field due to climatic variations.

Rao et. al., [7] proposed an expansive soil rating system, termed as the "Expansive Soil Index" (ESI). The model was developed as a function of using the soil properties most correlated with shrink–swell potential, swell index, liquid limit, and cation exchange capacity (CEC). The model gave expansive soil potential ratings (ESI) for each soil series.

Zumrawi [8] studied the swelling potential of compacted expansive soil and its relation with the soil state (water content, dry density, void ratio and the surcharge pressure) and the soil type (plasticity index and clay content). The study revealed a linear relationship of the swelling potential and the initial factor represented by soil state and the soil type. The coefficients of the linear relationship (constant and slope) were found to depend on the clay content, plasticity index and surcharge pressure.

In this paper, a method of treatment of swelling of expansive soil is presented. The method is simply based on the embedment of a geogrid in the soil. The geogrid is extended continuously inside the volume of soil where the swell is required to be controlled and orientated in the direction of swell.

Different research parameters are studied like geogrid stiffness, type of geocell fill and swelling potential of clay. Geocell grid columns of diameter 50 mm are inserted through the swelling soils and encased with geogrids of different stiffnesses.

2. Experimental Work, Materials and Procedures

The experimental work that has been conducted to validate the proposed method for treatment of swelling soil can be performed using a large scale model represented by model tests carried out in a test tank manufactured of a steel frame; the container is sufficiently rigid and exhibits no lateral

deformation during the preparation of the bed of soil and during the tests. This model is provided with three threaded holes along depth of tank to measure pore water pressure using pore water pressure transducers. Three dial gages were used to measure the swell occurring in three points; one point is lying on the footing and the other two gages measure the movement of two points lying 200 mm away from footing.

Soils with different swelling potentials were employed in this research. Bentonite-based Na and Bentonite-based Ca samples were brought from Karkuk city in Iraq, while the non-expansive soil was Kaolinite. Another type of soil sample was prepared in the laboratory by mixing 30% of Kaolinite with 70% Bentonite-based Na. Standard tests were performed to determine the physical and chemical properties of each soil.

There are two main types of bentonite the Na-bentonite and the Ca-bentonite, the first one has the greatest ability to swell [9].

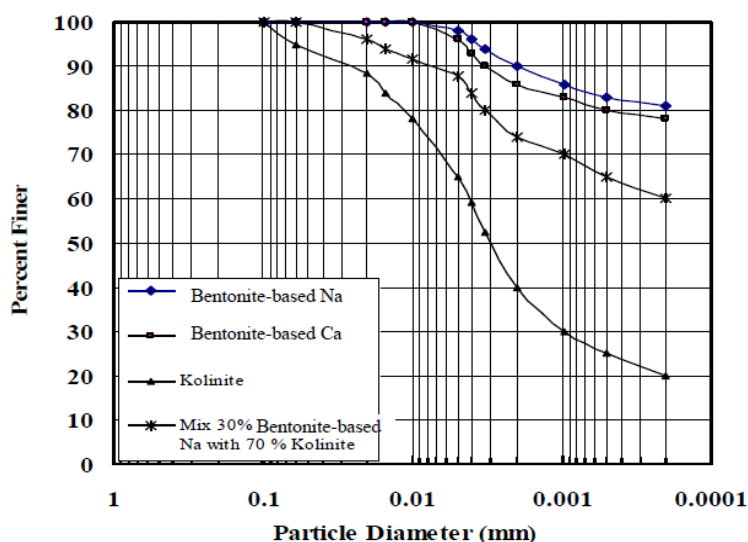
Details of the properties and the designation are given in Tables 1 and 2. The grain size distribution of the soil used is shown in Figure 1. According to the Unified Soil Classification System; all the soils are classified as (CH) fat clay.

Table 1. Physical properties of the soil used in the experimental work.

Samples Designation	Test Method	Sample 1 (S1)	Sample 2 (S3)	Sample 3 (S2)	Sample 4 (S4)
Description		Bentonite-based Ca	Bentonite-based Na	30% Kaolinite 70% Bentonite-based Na	Kaolinite
L.L%	ASTM D4318-00	125	155	130	45
P.L %	ASTM D4318-00	46	55	48	26
P.I %		79	100	82	19
Max. Dry density (gm/cm ³) by modified compaction test	ASTM D1557-99T	1.46	1.44	1.58	1.83
Max. Dry density (gm/cm ³) by standard compaction test	ASTM D698-99T	1.37	1.35	1.5	1.77
Max. Dry density (gm/cm ³) by static compaction test		1.268	1.275	1.35	1.72
W _{opt.} %, optimum moisture content @ Max. dry density by modified compaction test		23	25	20	12.5
W _{opt.} % @ Max. dry density by standard compaction test		25	28	22	15
W _{opt.} % @ Max. dry density by static compaction test		20	20	20	20
Specific gravity, G _s	BS 1377:1990 [16]	2.75	2.78	2.70	2.63
% Finer than 0.005 mm		95	97	88	65
*Activity %		0.83	1.031	0.91	0.76
$\text{Activity \%} = \frac{PI}{\% \text{ Finer than } 0.005 \text{ mm}}$					

Table 2. Chemical properties of the soils used in the experimental work.

Type of Sample	SO ₃ (mg/liter)	Gypsum content (mg/liter)	Total dissolved salts TDS (mg/liter)	pH value	Chloride Cl ⁻¹ mg/liter
Bentonite-based Ca (S ₁)	2.05	4.4075	1650	8.2	350
Bentonite-based Na (S ₃)	3.1	6.665	1775	8.4	625
30% Kaolinite 70% Bentonite base-Na (S ₂)	1.675	5.2	1731	8.3	514
Kaolinite (S ₄)	0.8	1.72	1628	8.2	250
Test method	BS 1377		Earth Manual, E8	BS1377 Test11(A)	BS812:Part4 1976

**Figure 1.** Grain size distribution for the clay soil used.

Chemical analysis was conducted to determine the chemical composition. The qualitative X-Ray diffraction was conducted on samples to get an idea about the mineralogical composition of the swelling soil samples. The mineralogical compositions of the soil, using the X-Ray diffraction method, are presented in Table 3.

Table 3. X-Ray diffraction results of testing soils.

Sample type	Clay Minerals
Sample 1 (S ₁) Bentonite-based Ca	Calcium Oxide (CaO), Silicon Oxide (SiO ₂)
Sample 3 (S ₂) 30% Kaolinite 70% Bentonite-based Na	Sodium Aluminum Silicate Hydrate, Silicon Oxide
Sample 2 (S ₃) Bentonite-based Na	Sodium Aluminum Silicate Hydroxide Hydrate NaO ₃ AL ₂ (Si ₁ AL) ₄₀ 10(OH) ₂ .2H ₂ O
Sample 4 (S ₄) Kaolinite	Silicon Oxide, SiO ₂

For the soils used (S₁, S₂, S₃), the swelling potential corresponding to plasticity indices 79%, 82%

and 100% is found to be very high according to [3] as indicated in Table 4.

Table 4. Typical soil properties versus expansion potential (Day, 1994).

Expansion Potential	Very low	Low	Medium	High	Very high
Clay content (< 2 μm)	0-10%	10-15%	15-25%	25-35%	35-100%
Plasticity index	0-10	10-15	15-25	25-35	> 35

Sand fill

Sand is used in the geocell grid columns. The sand is poorly graded of uniform size. The physical properties of the sand were determined according to ASTM (D422-01) [10] standard as presented in Table 5. The placing density of sand in the model box as a filter or in the hole of the geocell was achieved by raining technique. To obtain the desired density, different values of placing density were given by different heights of sand drop. The height of drop of 15 cm was chosen to maintain a placing unit weight of 15.2 kN/m³ which is corresponding to a value of the void ratio and relative density of 0.70 and 26 %, respectively.

Table 5. Physical and chemical properties of the used sand fill.

Index property	Test Method	Index value
Max. dry unit weight (kN/m ³)		17.4
Min. dry unit weight (kN/m ³)		14.4
Dry unit weight used (kN/m ³) at $D_r = 26\%$		15.2
e_{\min}		0.59
e_{\max}		0.82
e_{used} at dry unit weight used		0.70
Specific gravity (Gs)	ASTM D 854-2005	2.63
Coefficient of uniformity (Cu)		3.15
Coefficient of curvature (Cc)		1.07
T.S.S (%)	Earth Manual, E8	15.7
SO ₃ (%)	BS 1377	3.121
Organic matter (%)	BS 1377 -Test 8	1.46
Relative density (D_r %)	ASTM D2049-64T	26
Angle of internal friction (ϕ°) at $D_r = 26\%$	Direct-shear test	28°

Geogrid reinforcement

The geogrids used are polymer meshes commercially known as Netlon CE 121(G1) and Tensar SS2 geogrid (G3). Figure 2 shows the geogrid reinforcement used.



Figure 2. Geogrid tubes.

Testing Program

To investigate the swell, shrink and partial shrinkage, loading behavior with pore water pressure measurements and other phenomena for untreated soils in comparison with their counterparts of treated soils, model tests were conducted for this purpose. Each soil bed is compacted at the dry side of maximum dry density and water content using the static compaction.

The optimum moisture content and the dry unit weight of soil are very important for construction specification of soil improvement by compaction. Standard Procter compaction, modified compaction and static compaction are employed using the CBR mould for each swelling soil sample in the experimental work to investigate the effect of compaction method on the values of dry density, water content and the expected swelling results.

In the present work, the compaction characteristics of the soils are obtained using “standard” compaction test according to (ASTM D698-66T), and “modified” compaction test according to (ASTM D698) as well as static compaction.

The results are demonstrated in Table 1 using the Procter compaction mould and CBR mould which indicate that the maximum dry density of the soil reached uniform and repeatable when compacted by static method.

The bed of soil was prepared using static compaction at a water content of 20% and a stress of 300 kg to develop the corresponding maximum swell and maximum dry density.

Secondly, the variation of shear strength is measured using a Load Ring Penetrometer device at different liquidity indices.

According to Figure 3, the bed of soil was prepared at water content of 20 % corresponding to liquidity index in the range of 20 % to maintain an undrained shear strength of 17.5 kPa for sample S₂ and 21 kPa for sample S₃.

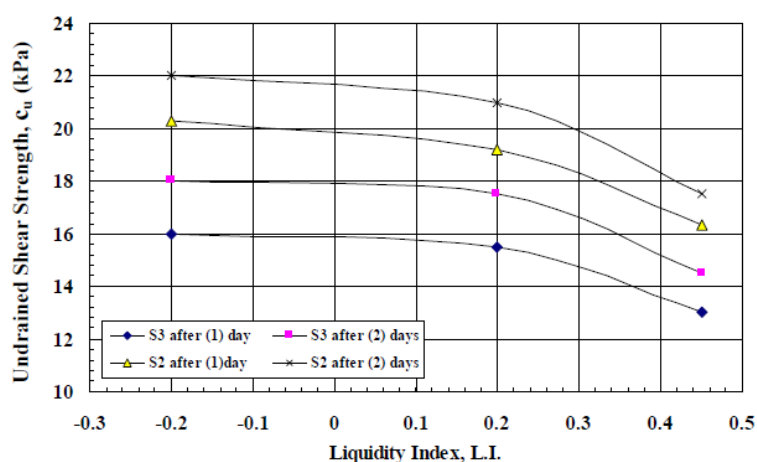


Figure 3. Variation of undrained shear strength with liquidity index at different times.

Placement of the bed of soil

Each 25 kg of soil sample was mixed with enough quantity of water to get the desired consistency. The wet soil was kept inside tightened polythen bags for a period of two days. This period was sufficient to get uniform moisture content. After that, the soil was placed in three layers inside a steel container of (800×200) mm and 600 mm in height. Before that, the sides of the container were coated with silicone grease to minimize the friction effect. After the placement of each layer, it was pressed gently with a wooden tamper of size 75×75 mm in order to remove entrapped air. After completing each layer, the top surface was scraped, levelled and compressed by a steel sheet 790×190 mm loaded from axial loading system to reach the bed of soil and left for a period of two days to regain part of its strength.

Construction and installation of geogrid encased sand columns

All the sand columns have a diameter of 50 mm, length to diameter ratio ($L/D = 6$) with spacing of 2 times the footing width (B).

Then, a geogrid cell (Figure 2) was inserted into the column hole using a hollow steel pipe with internal diameter of 50 mm. The sand was poured into the hole in layers and compacted gently by a tamping rod. After pouring all the specific amount of sand, the full depth of the hole was filled with sand at a dry unit weight of 15 kN/m^3 .

Testing Procedure

The general view of the testing ring employed in the present research is illustrated in Figure 4. The ring has the capability to sustain the applied load to simulate the stresses occurring under plate or pile load test. An experimental formulation based on an approximate tenth 10^{th} scale for general square footing was adopted in this work. A square footing model with dimensions of $100 \times 100 \text{ mm}$ was used. The length of grid geocell columns was 300 mm embedded inside the swelling soil.



Figure 4. General view of the large scale model.

The pressure applied to the model was measured using a load cell connected to the readout pressure system; the information was recorded at selected intervals of time in a data file in the computer along with the reading signals of pore water pressure transducers. The entire testing process was run with the aid of computer software.

The displacement of the soil model was measured using three dial gages; one is placed on the footing and the others are placed at a distance of 200 mm away from the footing on the geocells located right and left the footing.

The other side of container model has three threaded holes; each is 10 mm diameter in order to accommodate the pore water pressure transducers and the de-airing equipment of the pore water pressure system as shown in Figure 5.

To simplify the observations of the soil samples, geogrid types and grid geocell columns that will be dealt with in the experimental work, symbols are used to characterize each model. Table 6 shows each model and its symbol.

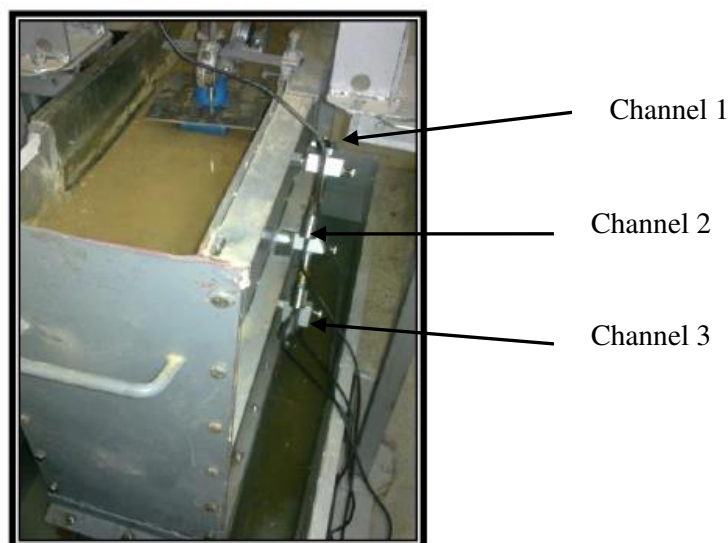


Figure 5. Pore water pressure measurement system.

Table 6. Model types and their symbols.

Sample type	Sample symbol
Bentonite-based Ca sample	S1
Mixture 70% Bentonite-based Na sample with 30% Kaolinite	S2
Bentonite-based Na sample	S3
Geogrid No. 1 (stiffness = 120 kN/m)	G1
Geogrid No. 2 (stiffness = 40 kN/m)	G2
Geogrid No. 3 (stiffness = 240 kN/m)	G3
Geocell filled with the same soil	F1
Geocell filled with sand	F2

3. Results and Discussion

Swell-time relationships

A relatively large scale model was used to estimate the swell-time relationship for different types of soils of different plasticity indices before and after treatment.

Table 7 graphically describes the locations of the measurement points in the model. The measured swell and pore water pressure are plotted against time for samples with and without treatment (using geocell filled with the same soil or sand). The results are demonstrated in Figures 6 to 11.

It can be seen that the expansive soils takes long period of time to complete their expansion, therefore the testing time of 27 days was chosen for all test groups.

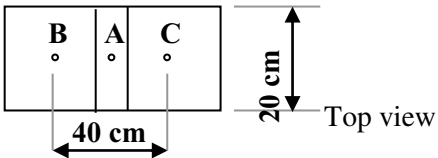
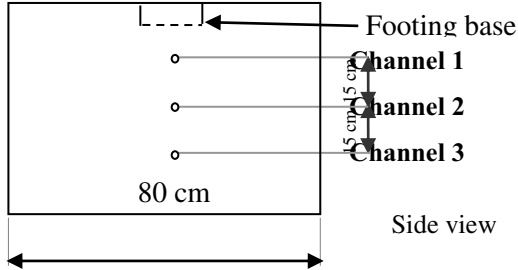
Figures 6 to 8 present the results for S3 soil sample model with and without treatment with pore water pressure records while Figures 9 to 11 for S2 sample model with and without treatment. From the results, the effective method for treatment can be summarized by presenting the amount of decrease in the measured swell and the activity of geocell grid columns in restricting the soil swelling due to increase of the interlocking between the geocell with fill material.

It can be noticed that the changes in pore water pressure during swelling process are small; the pore water pressures are negative especially at the top and bottom of the model indicating that matric suction is related to swelling.

The largest value for variations in matric suction occurs near the ground surface of the soil samples. The matric suction measurements indicate low values that can be attributed to the conditions of the soil sample tested; the soil sample is compacted at optimum moisture content during static

compaction. In addition, there is no way to dissipate the air pressure along the soil sample depth during soaking of the soil sample from top and bottom sides in the model. This is clear especially in data measured in channel 2.

Table 7. Geocell locations and descriptions of measuring points in the model.

Point symbol	Description of measuring points	Measuring points location details
A	Lies below middle of footing.	
B and C	Lies at 20 cm distance on both sides of point A.	
Channel 1 Channel 2 Channel 3	High point in the box. Medium point in the box. Low point in the box.	

The effect of treatment is clear from the results which reflect the effectiveness of geocells in restricting the soil movement. This finding is in agreement with the results of [11] who indicated that the displacement field in foundation is changed significantly as a result of reinforcement.

The mineralogical model for the variations of the pore water pressure with time dependent swell behavior may be more appropriate because the ingress of water between the plates in clay crystal is not controlled by effective stress, but by the physicochemical reactions taking place between the plates. These physicochemical reactions are controlled by the osmotic suction caused by the presence of exchangeable cations between the plates, and are therefore only indirectly influenced by the matric suction prevailing in the pores between the clay crystals, [12]. Therefore, the pore water pressure (matric suction) at the top and bottom has considerable difference at the beginning and end of all tests. The method of treatment increased the dissipation of pore water pressure by increasing the void channels and permeability of soil sample especially with the use of geocell cylinders filled with sand.

The same results were obtained for S2 soil sample model. Figures 9 to 11 display the effectiveness of the method of treatment as indicated in the testing results. The figures also demonstrate the effect of soil plasticity on the magnitude of improvement. When geocells are filled with sand which has low plasticity, the treatment method is found to be more effective than the case of geocells filled with clay.

From these results, the method of geocell embedment technique is affirmed to be successful as expressed by the improvement factors listed in Table 8. The improvement factors vary from 19 to 64 based on the plasticity index and type of fill material.

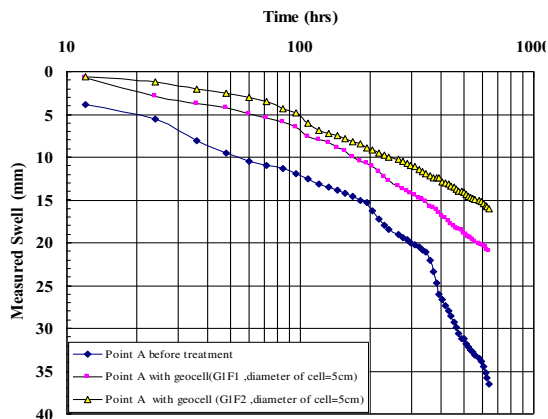


Figure 6. Swell measured at point A before and after treatment of S3 model beneath square footing.

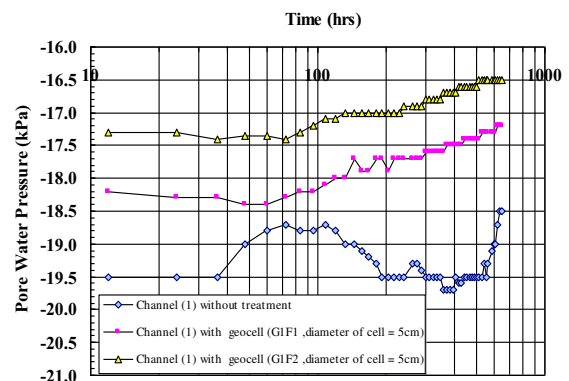


Figure 7. Pore water pressure at channel (1) before and after treatment of S3 model beneath square footing.

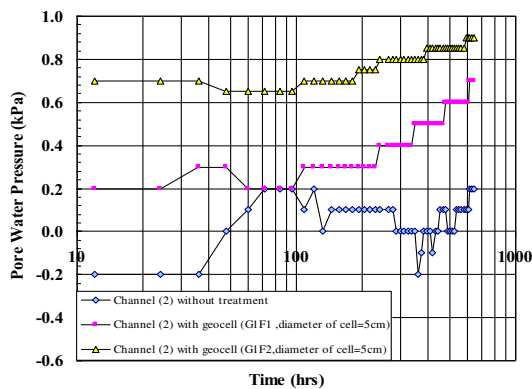


Figure 8. Pore water pressure at channel (2) before and after treatment of S3 model beneath square footing.

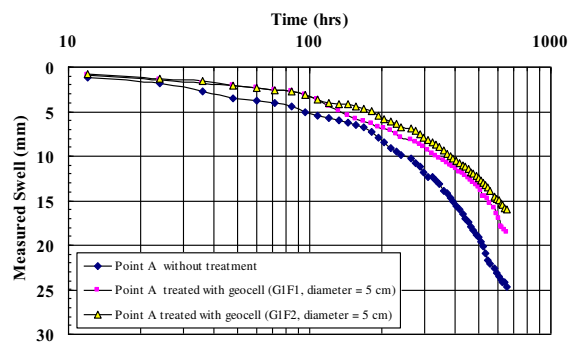


Figure 9. Swell measured at point A before and after treatment of S2 model beneath square footing.

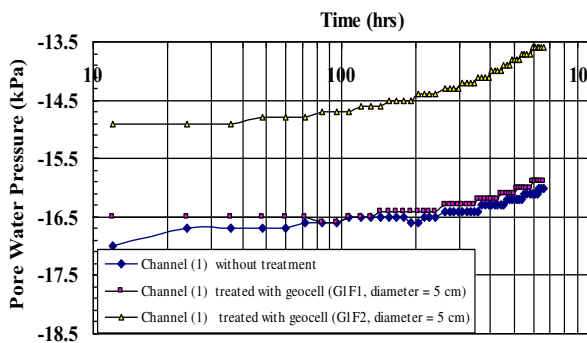


Figure 10. Pore water pressure at channel (1) before and after treatment of S2 model beneath square footing.

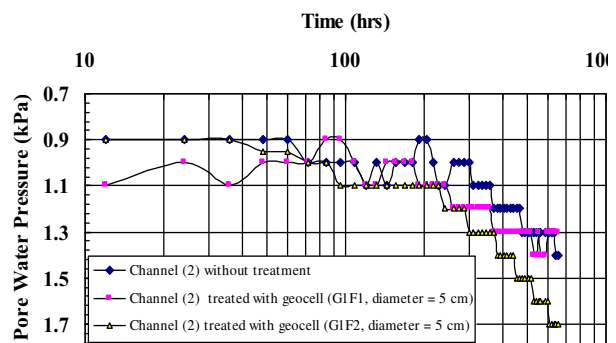


Figure 11. Pore water pressure at channel (2) before and after treatment of S2 model beneath square footing.

Table 8. Improvement factors for different samples treated by using geocells of different fill materials, stiffness of geocell is 120 kN/m.

Sample symbol model	Dry density by static compaction test (gm/cm ³)	Measuring point	Type of fill material	IF (%)
S2	1.35	B	the same soil	19
S2	1.35	B	sand	35.3
S3	1.275	B	The same soil	42
S3	1.275	B	sand	64

Effect of fill material

Figures 12 and 13 are drawn to study the effect of fill material on the effectiveness of the proposed method of treatment. Geocell material creates effective channels which support the basic work of the treatment method by increasing the permeability and reduction in soil matric suction.

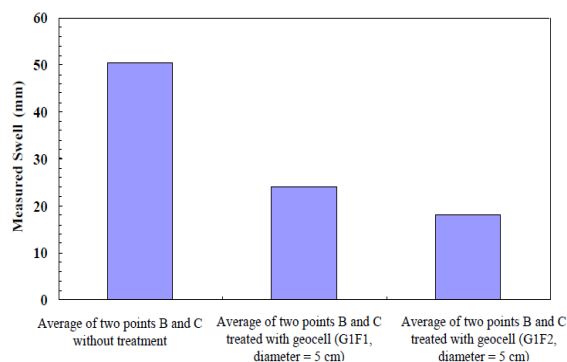
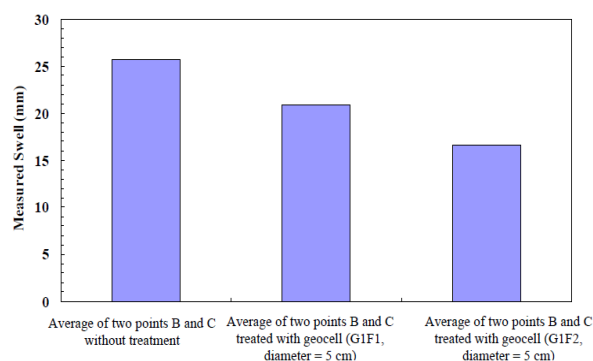
**Figure 12.** Effect of fill material on geogrid treatment for S3 soil sample model beneath square footing.**Figure 13.** Effect of fill material on geocell treatment for S2 soil sample model beneath square footing.

Table 8 presents the results of the effect of fill material on the recorded results. From the results, the use of geocell filled with the same expansive soil causes a decrease of about 19 % and 42 % in the final swell for S2 and S3 soils, respectively whereas filling the cell with sand causes a decrease of about 35.3 % and 64 % in the final swell reduction for S2 and S3 soils, respectively.

Sand fill material accelerates the flow of water through the soil sample model; therefore the treatment with geocell filled with sand is more effective. In addition, the area of clay in contact with footing is reduced. The sand in the pockets forms a better composite material and the geocell behaves as a stiffer bed that redistributes stress over a wider area giving an increase in the bearing capacity and a reduction in the settlement of the footing as outlined by [13].

For the treated soils, the geogrid reinforced column with fill materials works like a pile structure and sustain the applied pressure for the whole soil. Therefore, the mechanical behavior of the treated soil is different from any chemical additive behavior. The aim of using the mechanical treatment by geogrid reinforced column is to restrict the soil swell in the direction of movement during wetted or dry season, the same principle is controlling when the swelling soil is under tension stress due to swelling pressure or under compression stress by consolidation pressure [14].

Effect of geocell stiffness

To demonstrate the effect of geocell stiffness on the treatment method, G1 and G3 types of geogrid are

chosen to show the effect of the variation in stiffness of the geocell on the measured swell.

The relationships of the final swell and pore water pressure with time are plotted in Figures 14 and 15. The results suggest that increasing the stiffness lead to an increase in the restraint and decrease in matric suction of swelling soil.

It is concluded that, the geocell stiffness has a little effect on the pore water pressure, which can be due to no change in the conditions of the model situations as a result of this fact; there is no change in the matric suction. Also the degree of saturation in the model is not homogenous in the vertical direction during the test period of 27 days; the effect of stiffness may be more pronounced if the soil model is allowed to swell until full saturation of the whole soil.

Figures 14 to 17 show a comparison of swelling measured at two points with geocell stiffness variation. improvement factors obtained in the present work are given in Table 9. The amount of improvement factor increases with increasing the grid stiffness. The geocells used in experiments included in this table are 5 cm in diameter filled with sand.

The effect of the elastic modulus of the geogrid on the swelling, pore water pressure, and degree of saturation decreases slightly when the elastic modulus increases. Subsequently, the effect diminishes gradually with the depth. The stiffness of the geogrid leads to the restriction of soil movement and the concentration of stresses within the geocell, hence decreasing the swelling and pore water pressure [15].

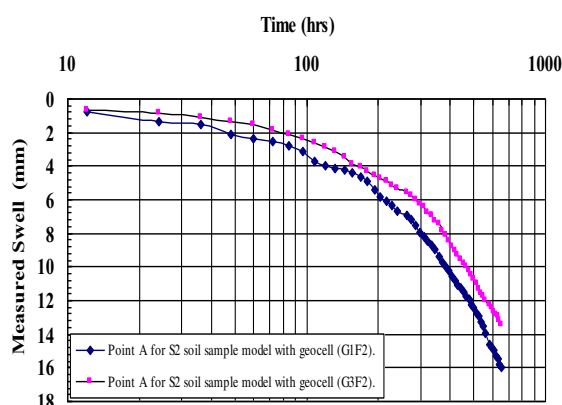


Figure 14. Effect of geocell stiffness on the swelling for S2 soil sample model measured at point A beneath square footing.

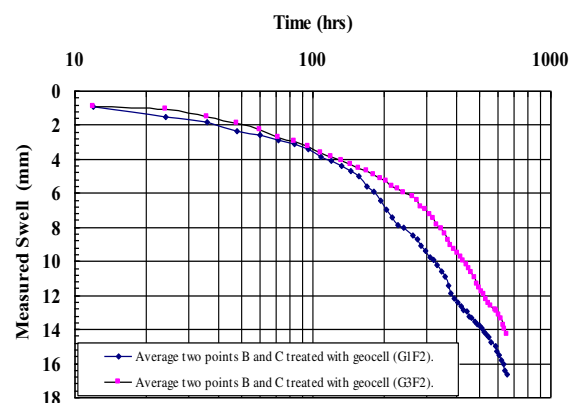


Figure 15. Effect of geocell stiffness on the swelling for S2 soil sample model measured as an average of two points B and C beneath square footing.

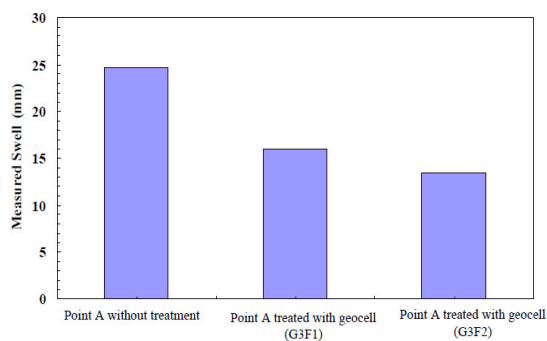


Figure 16. Effect of geocell of stiffness on the swelling for S2 soil sample model at point A beneath square footing.

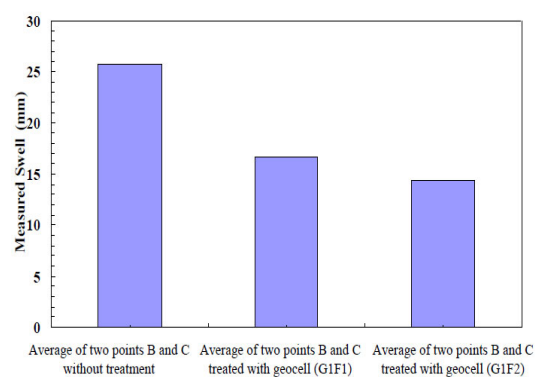


Figure 17. Effect of geocell stiffness on the swelling for S2 soil sample model at average two points B and C beneath square footing.

Table 9. Improvement factors indicating the effect of geocell stiffness on the obtained reduction in swell.

Stiffness of geocell (kN/m)	Measuring points	IF (%)
120	A	35.3
240	A	45.6
120	B	35.3
240	B	44.3

4. Conclusions

The main points concluded from the experimental work can be summarized as follows:-

1. The treatment of swelling soil using grid geocells filled with sand or the same soil is found to be effective. If the geocell is filled with the same expansive soil, it causes a decrease of about 19 % and 42 % in the final swell for S2 and S3 soils, respectively, whereas filling the cell with sand causes a decrease of about 35.3 % and 64 % in the final swell reduction for S2 and S3 soils, respectively.
2. Swelling test in the model reveals promising results of the proposed treatment technique. The improvement factors, IF, range between (30 to 60) % depending on the geogrid stiffness, soil plasticity, fill material (sand or clay), dry density of sand fill and clay percentage of the fill material.
3. The geocell has a significant effect on the experimental results. The reduction in swell increases with increasing the geogrid stiffness and when using sand as a fill material, the reduction is apparently due to a strong interference bond which restricts the relative movement between the clay and the grid. The sand fill material accelerates the flow of water through the soil sample model; therefore, the treatment with geocell filled with sand is more effective.
4. The treatment method shows the activity of geocell fill material in reducing the matric suction (pore water pressure). When sand is used, a new channel is created for dissipation of pore water pressure. The pore water pressure is slightly changed because the swelling soil needs a long period to complete the swelling and reach a saturation state. This change is sensed near the top surface and near the bottom and both location points are near the flooding water. The geocell fill material increases this change because the sand materials accelerate the water migration.

References

- [1] Katha, B. R., 2002 *Shrinkage strain characterization of expansive soils using digital imaging technology*, M.Sc. Thesis (The University of Texas at Arlington, Texas)
- [2] Chen, F.H., 1988 Foundations on expansive soils *Developments in Geotechnical Engineering*, Vol. 12 (Elsevier Publications, the Netherlands)
- [3] Day, R.W., 1994 Swell-shrink behavior of compacted clay *Journal of Geotechnical Engineering ASCE* **120** 618–623
- [4] Al-Omari, R. R., and Hamodi, F. J., 1991 Swelling resistant geogrid-a new approach for the treatment of expansive soils *Geotextiles and Geomembranes* **10** 295-317
- [5] Al-Homoud, A. S., Husein M. B., and Al-Bashabshah, M. A., 1995 Cyclic swelling behavior of clays *Journal of Geotechnical Engineering ASCE* **121** 562–565
- [6] Mitchell, J.K., 1993 *Fundamentals of soil behavior* (John Wiley and Sons, New York)
- [7] Rao, S.M., Thyagaraj, T., and Thomas, H.R., 2006 Swelling of compacted clay under osmotic gradients *Geotechnique* **56** 707-713
- [8] Zumrawi, M. E. 2013 Swelling potential of compacted expansive soils *International Journal of Engineering Research and Technology (ISERT)* **2** 1-6
- [9] Athanassopoulos, C., 2011 Natural sodium versus activated calcium bentonite in geosynthetic clay liners (GCLs) *Solid Waste and Recycling Conference*, available at URL:<http://www.nyfederation.org/PDF2011/04> , Athanassopoulos.

- [10] ASTM D422-2001 *Standard test method for particle size-analysis of soils* (American Society for Testing and Materials, West Conshohocken, Pennsylvania, USA)
- [11] Wang Wei's, 2000 Study on model tests and mechanism of soft soil foundation reinforced by geotextile *Chinese Journal of Geotechnical Engineering* **22** 750-753
- [12] Saxena, K.R., 1994 *Geotechnical engineering-emerging trends in design and practice* (A.A Balkema, Rotterdam) pp. 33-36
- [13] Moghaddas, S.N., and Dawson, A.R., 2010 Comparison of bearing capacity of a strip footing on sand with geocell and with planar forms of geotextile reinforcement *Geotextiles and Geomembranes* **28** 72–84
- [14] Fattah, M. Y., Al-Omari, R. R., Ali, H. A., 2015 Numerical Simulation of the Treatment of Soil Swelling Using Grid Geocell Columns *Slovak Journal of Civil Engineering* **23** 9–18, DOI: 10.1515/sjce-2015-0007.
- [15] Al-Omari, R. R., Fattah, M. Y., Ali, H. A., 2016 Treatment of Soil Swelling Using Geogrid Reinforced Columns *Italian Journal of Geosciences* **135** 83-94, doi: 10.3301/IJG.2014.54.
- [16] B.S. 1377 1990 *Methods of test for soils for civil engineering purposes* (British Standards Institution)